Robotica (2008) volume 26, pp. 255–266. © 2007 Cambridge University Press
doi:10.1017/S0263574707003840 Printed in the United Kingdom

Stability of Two-Dimensional Blind Grasping under the Gravity Effect and Rolling Constraints

S. Arimoto*†, M. Yoshida† and J.-H. Bae‡

† *RIKEN, Bio-Mimetic Control Research Center, Nagoya, Aichi, 463-0003 Japan*
‡*Pohang Institute of Intelligent Robotics, San 31, Hyoja-Dong, Nam-Gu, Pohang, Gyeongbuk 790-784, S. Korea.*

(Received in Final Form: May 1, 2007. First published online: September 28, 2007)

SUMMARY
This paper aims to show a sensory-motor coordination control scheme that realizes stable pinching of rigid objects with parallel or nonparallel flat surfaces movable in 2-dimensional vertical plane by a pair of robot fingers with hemispherical ends. The proposed control signal is composed of gravity compensation for fingers, damping shaping, exertion of forces to the object from opposite directions, generation of moments for balancing of rotational moments, and regressors for estimating unknown steady-state terms, all of which neither need the knowledge of object parameters nor use any object sensing data. In other words, stable grasping can be realized by using only finger-joint sensing in a blind manner without using force sensors or tactile sensing. Stability of pinching motion with convergence to the state of force/torque balance is shown through computer simulations and is also proved theoretically.

KEYWORDS: Multifingered hand; Blind grasping; Force/torque balance; Sensory-motor coordination; Bernstein's DOF problem.

1. Introduction

Human manipulates an object by using three or four fingers with multi degrees of freedom (DOF) in one hand. However, use of three or four fingers is redundant in general for manipulation of the object. This redundancy incurs the well-known annoying problem of ill-posedness of inverse kinematics and used to prevent us from attacking interesting problems of design of controllers for dynamic grasping and object manipulation. This is really a difficult problem in robotics research; as discussed by Bicchi.[1] A famous text book[2] also pointed out the difficulty in such a way that

> The study of human biological motor mechanisms led the Russian psychologist Bernstein to question how the brain could control a system with so many different degrees of freedom interacting in such a complex fashion. Many of these same complexities are also present in robotic systems and limit our ability to use multifingered hands and other robotic systems to their full advantage.

* Corresponding author. E-mail: arimoto@se.ritsumei.ac.jp

Notwithstanding these arguments, it is recently clarified that human-like pinching with stable grasp and manipulation of an object can easily be established by sensory feedback control with the aid of rolling contacts between the hemispherical finger ends and the object surfaces, even though the total DOF of the overall fingers-object system is higher than the number of physical variables necessary and sufficient for description of a target task.[3–6] The essentials of this new control scheme are (1) with use of rolling contacts that exert tangential constraint forces to the object, (2) without use of force and tactile sensings, (3) without knowing physical parameters of the object and location of the object mass center, and (4) finding of sensory–motor coordination signals simply calculated from the knowledge of only finger kinematics, measurement data on finger joints and measurement of the rotational angle of the object relative to the vertical line or a prefixed axis. However, we observe in everyday life that human can pinch an arbitrary object by using a pair of thumb and index (or middle) finger while their eyes are closed, if the pair of such fingers is preshaped and reaching closely to the object. Such a problem of blind pinching was first attacked in our previous paper[7] in the case that motion of the overall fingers–object system is confined to horizontal plane and thereby it is not affected by the gravity force. On the other hand, it is known that many of human fast and voluntary limb movements such as multijoint reaching, grasping an object bilaterally, etc. are produced in a feedforward manner without sensory feedbacks except spinal reflex loops,[8] provided the movements have been well practiced and sufficiently skilled. Movements of human skilled pinching must be generated feedforwardly without use of any external sensings such as visual or tactile sensings, as claimed in physiology[8] and predicted from various observations obtained in developmental psychology.[9]

This paper challenges a problem of blind grasp with dynamic stability converging to the form of force/torque balance for a rigid object with parallel or nonparallel surfaces under the effect of gravity. It is assumed that motion of a pair of robot fingers with two or three DOF and the object is confined to a vertical plane and finger ends are hemispherically shaped. It is shown through computer simulations and also proved theoretically that proposed control signals calculated in real-time from only finger parameters and measurement data on only finger joints lead to asymptotic convergence of the solution trajectory to a still state satisfying the form of force/torque balance.

https://doi.org/10.1017/S0263574707003840 Published online by Cambridge University Press

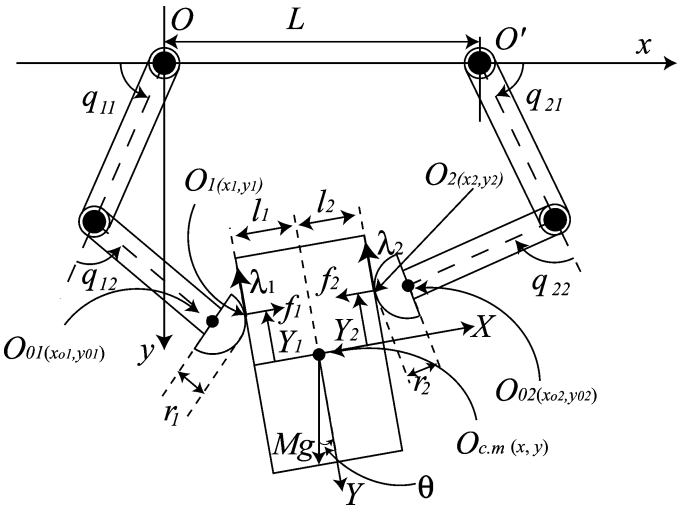


Fig. 1. A pair of robot fingers pinching a rigid object.

2. Dynamics

First, the dynamics of a pair of two DOF finger robots and a 2D object with flat surfaces are derived. The coordinates system of the overall system is shown in Fig. 1. Vector $\boldsymbol{q}_1 = (q_{11}, q_{12})^{\mathrm{T}}$ denotes the joint angles of the left hand side finger and vector $\boldsymbol{q}_2 = (q_{21}, q_{22})^{\mathrm{T}}$ denotes those of the right finger. The fingertips are rigid and hemispherically shaped with radius r_i. The mass center of the object is denoted by $O_{\mathrm{c.m.}}$. We define vector $\boldsymbol{w} = (x, y, \theta)^{\mathrm{T}}$ in the coordinates system $\{O\text{–}\mathbf{xy}\}$, where $\boldsymbol{x} = (x,y)^{\mathrm{T}}$ denotes the position of the object mass center and θ is the rotational angle of the object. The symbols l_{ij},m_{ij}, and $I_{ij}(i, j = 1, 2)$ denote length, mass, and inertia moment of link j of finger i, respectively. The symbols M and I denote mass and inertia moment of the object, respectively, and L the distance between the origin$\{O\}$ of the left finger and the origin$\{O^{'}\}$ of the right finger.

The distance Y_i between the contact point and the object surface point at which the straight line from the mass center $O_{\mathrm{c.m.}}$ crosses the object surface perpendicularly, is shown in the following:

$$Y_i = (x_{0i} - x)\sin\theta + (y_{0i} - y)\cos\theta, \qquad i = 1, 2 \tag{1}$$

Where $(x_{0i}, y_{0i})^{\mathrm{T}}$ denotes the position vector of O_{0i}, the center of curvature of fingertip sphere as shown in Fig. 1, and θ denotes the orientation angle of the object relative to the y-axis as shown in Fig. 1. In this paper, we adopt the rule of positive angles (radian) in the counterclockwise direction except the joint angles $q_{2j}(j = 1, 2 \sim j = 1, 2, 3)$ of the right hand finger $i = 2$. The distance Y_i must be subject to the constraint such that the fingertip does not slip on the object surface, that is,

$$Y_i = c_{0i} - r_i\{\pi - (-1)^i\theta - q_{11} - q_{12}\}, \qquad i = 1, 2 \tag{2}$$

where c_{01} and c_{02} are constant. Then, R_1 and R_2 are defined as follows:

$$\begin{aligned} R_i &= (x_{0i} - x)\sin\theta + (y_{0i} - y)\cos\theta - c_{01} \\ &\quad + r_i\{\pi - (-1)^i\theta - q_{i1} - q_{i2}\} = 0, \qquad i = 1, 2 \end{aligned} \tag{3}$$

These constraints lead to introduction of the scalar R in the following way by using Lagrange multipliers λ_1 and λ_2 (tangent forces).

$$R = \lambda_1 R_1 + \lambda_2 R_2 \tag{4}$$

It is easy to calculate partial differentials of $R_i(i = 1, 2)$ in $\boldsymbol{q}_i$ as follows:

$$\frac{\partial R_i}{\partial \boldsymbol{q}_i} = J_i^{\mathrm{T}} \begin{pmatrix} \sin\theta \\ \cos\theta \end{pmatrix} - r_i \boldsymbol{e}_i, \qquad i = 1, 2 \tag{5}$$

where $\boldsymbol{e}_i = (1, 1)^{\mathrm{T}}$ and J_i denotes the Jacobian matrix defined as:

$$J_i^{\mathrm{T}} = \begin{pmatrix} \dfrac{\partial x_{0i}}{\partial \boldsymbol{q}_i} & \dfrac{\partial y_{0i}}{\partial \boldsymbol{q}_i} \end{pmatrix} \tag{6}$$

The constraint of the fingertip so that it is stuck to the object is shown by the following geometric relation:

$$\begin{aligned} Q_i &= -(l_i + r_i) - (-1)^i\{(x - x_{0i})\cos\theta \\ &\quad - (y - y_{0i})\sin\theta\} = 0, \qquad i = 1, 2 \end{aligned} \tag{7}$$

In the same way, we obtain the followings:

$$\frac{\partial Q_i}{\partial \boldsymbol{q}_i} = (-1)^i J_i^{\mathrm{T}} \begin{pmatrix} \cos\theta \\ -\sin\theta \end{pmatrix}, \qquad i = 1, 2 \tag{8}$$

These constraints represent the scalar Q in the following way by using Lagrange multipliers f_1 and f_2 (grasping forces).

$$Q = f_1 Q_1 + f_2 Q_2 \tag{9}$$

Referring to the previous paper[3] by defining the Lagrangian $L = K + R + Q - P_1 - P_2 - Mgy$ where $K = (1/2)\sum \dot{\boldsymbol{q}}_i^{\mathrm{T}} H_i(\boldsymbol{q}_i)\dot{\boldsymbol{q}}_i + (1/2)(M\dot{x}^2 + M\dot{y}^2 + I\dot{\theta}^2)$ with finger inertia matrix $H_i(\boldsymbol{q}_i)$ stands for the total kinetic energy and P_i for the finger potential energy, we obtain dynamic equations of the overall system as follows:

$$\begin{aligned} &\left\{H_i(\boldsymbol{q}_i)\frac{\mathrm{d}}{\mathrm{d}t} + \frac{1}{2}\dot{H}_i(\boldsymbol{q}_i)\right\}\dot{\boldsymbol{q}}_i + S_i(\boldsymbol{q}_i, \dot{\boldsymbol{q}}_i)\dot{\boldsymbol{q}}_i + \boldsymbol{g}_i(\boldsymbol{q}_i) \\ &\quad - f_i\left(\frac{\partial Q_i}{\partial \boldsymbol{q}_i}\right) - \lambda_i\left(\frac{\partial R_i}{\partial \boldsymbol{q}_i}\right) = \boldsymbol{v}_i, \qquad i = 1, 2 \end{aligned} \tag{10}$$

$$\begin{cases} M\ddot{x} - \{f_1\cos\theta - f_2\cos\theta\} + \lambda_1\sin\theta + \lambda_2\sin\theta = 0 \\ M\ddot{y} + f_1\sin\theta - f_2\sin\theta + \lambda_1\cos\theta + \lambda_2\cos\theta - Mg = 0 \\ I\ddot{\theta} - f_1 Y_1 + f_2 Y_2 + \lambda_1 l_1 - \lambda_2 l_2 = 0 \end{cases} \tag{11}$$

where $S_i(\boldsymbol{q}_i, \dot{\boldsymbol{q}}_i)$ is skew-symmetric. Equation (10) is the motion equation of the fingers, and Eq. (11) is the dynamic equations of the object.

Second, the dynamics of a pair of three DOF finger robots and a 2D object with nonparallel flat surfaces are derived. The coordinates system of the overall system is shown in Fig. 2. The holonomic constraints in this case corresponding

https://doi.org/10.1017/S0263574707003840 Published online by Cambridge University Press

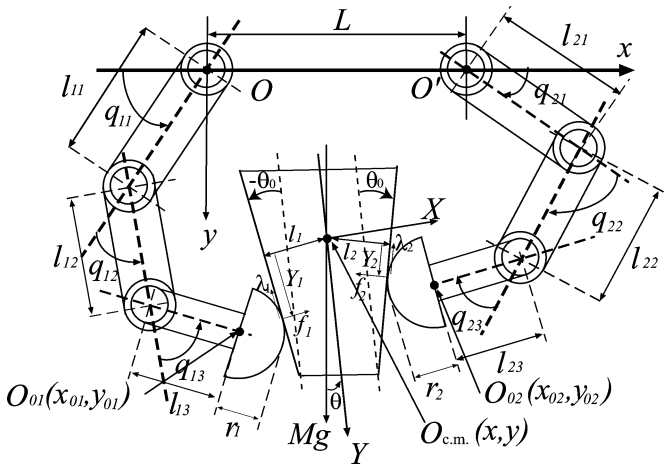


Fig. 2. A pair of robot fingers pinching a rigid object with nonparallel surfaces.

Table I. Explicit formulae of Q_i and R_i for an object with nonparallel flat surfaces.

Point contact constraint:

$$Q_i = -(l_i + r_i) - (-1)^i\{(x - x_{0i})\cos(\theta + (-1)^i\theta_0) - (y - y_{0i})\sin(\theta + (-1)^i\theta_0)\} = 0 \qquad i = 1, 2 \tag{T-1}$$

Rolling constraint:

$$R_i = Y_i - c_{0i} + r_i\left\{\pi - (-1)^i\theta - \theta_0 - \textstyle\sum_{j=1}^{3} q_{ij}\right\} = 0 \qquad i = 1, 2 \tag{T-2}$$

where

$$Y_i = (x_{0i} - x)\sin(\theta + (-1)^i\theta_0) + (y_{0i} - y)\cos(\theta + (-1)^i\theta_0), \qquad i = 1, 2 \tag{T-3}$$

to Eqs. (3) and (7) are given in Table I. In a similar way, it is possible to derive the following equation:[4]

$$\left\{H_i(\boldsymbol{q}_i)\frac{\mathrm{d}}{\mathrm{d}t} + \frac{1}{2}\dot{H}_i(\boldsymbol{q}_i)\right\}\dot{\boldsymbol{q}}_i + S_i(\boldsymbol{q}_i, \dot{\boldsymbol{q}}_i)\dot{\boldsymbol{q}}_i + \boldsymbol{g}_i(\boldsymbol{q}_i) - f_i\left(\frac{\partial Q_i}{\partial \boldsymbol{q}_i}\right) - \lambda_i\left(\frac{\partial R_i}{\partial \boldsymbol{q}_i}\right) = \boldsymbol{v}_i, \qquad i = 1, 2 \tag{12}$$

$$\begin{cases} M\ddot{\boldsymbol{x}} - \displaystyle\sum_{i=1,2}\left(f_i\frac{\partial Q_i}{\partial \boldsymbol{x}} + \lambda_i\frac{\partial R_i}{\partial \boldsymbol{x}}\right) - Mg\begin{pmatrix}0\\1\end{pmatrix} = 0 \\ I\ddot{\theta} - \displaystyle\sum_{i=1,2}\left(f_i\frac{\partial Q_i}{\partial \theta} + \lambda_i\frac{\partial R_i}{\partial \theta}\right) = 0 \end{cases} \tag{13}$$

where partial derivaties of Q_i and R_i $(i = 1, 2)$ with respect to $\boldsymbol{q}_i$, $\boldsymbol{x}$, and θ are given in Table II.

Table II. Explicit formulae of partial differentials of Q_i and R_i in q_i, $\boldsymbol{x}$, and θ for an object with nonparallel flat surfaces.

$$Q = f_1Q_1 + f_2Q_2 \qquad R = \lambda_1R_1 + \lambda_2R_2$$

$$\frac{\partial Q}{\partial \boldsymbol{q}_i} = f_i\left(\frac{\partial Q_i}{\partial \boldsymbol{q}_i}\right) = (-1)^i f_i J_i^{\mathrm{T}}(q_i)\begin{pmatrix}\cos(\theta + (-1)^i\theta_0)\\ -\sin(\theta + (-1)^i\theta_0)\end{pmatrix}, \qquad i = 1, 2 \tag{T-4}$$

$$\frac{\partial R}{\partial \boldsymbol{q}_i} = \lambda_i\left(\frac{\partial R_i}{\partial \boldsymbol{q}_i}\right) = \lambda_i\left\{J_i^{\mathrm{T}}\begin{pmatrix}\sin(\theta + (-1)^i\theta_0)\\ \cos(\theta + (-1)^i\theta_0)\end{pmatrix} - r_i\boldsymbol{e}_i\right\}, \qquad i = 1, 2 \tag{T-5}$$

$$\frac{\partial Q}{\partial x} = f_1\cos(\theta - \theta_0) - f_2\cos(\theta + \theta_0) \tag{T-6}$$

$$\frac{\partial R}{\partial x} = -\lambda_1\sin(\theta - \theta_0) - \lambda_2\sin(\theta + \theta_0) \tag{T-7}$$

$$\frac{\partial Q}{\partial y} = -f_1\sin(\theta - \theta_0) + f_2\sin(\theta + \theta_0) \tag{T-8}$$

$$\frac{\partial R}{\partial y} = -\lambda_1\cos(\theta - \theta_0) - \lambda_2\cos(\theta + \theta_0) \tag{T-9}$$

$$\frac{\partial Q}{\partial \theta} = f_1Y_1 - f_2Y_2 \tag{T-10}$$

$$\frac{\partial R}{\partial \theta} = -\lambda_1l_1 + \lambda_2l_2 \tag{T-11}$$

3. Control Signals

Now, we propose a class of control signals for blind grasping of a rigid object, which is defined as

$$\boldsymbol{v}_i = \boldsymbol{g}_i(\boldsymbol{q}_i) - c_i\dot{\boldsymbol{q}}_i + (-1)^i\frac{f_d}{r_1 + r_2}J_i^{\mathrm{T}}(q_i)(\boldsymbol{x}_{01} - \boldsymbol{x}_{02}) - \frac{\hat{M}g}{2}\left(\frac{\partial y_{0i}}{\partial \boldsymbol{q}_i}\right) - r_i\hat{N}_i\boldsymbol{e}_i, \qquad i = 1, 2 \tag{14}$$

where

$$\hat{M}(t) = \hat{M}(0) + \int_0^t \frac{g}{2\gamma_M}\sum_{i=1,2}\left(\frac{\partial y_{0i}}{\partial \boldsymbol{q}_i}\right)^{\mathrm{T}}\dot{\boldsymbol{q}}_i\mathrm{d}\tau = \hat{M}(0) + g\gamma_M^{-1}\left\{\frac{y_{01}(t) + y_{02}(t)}{2} - \frac{y_{01}(0) + y_{02}(0)}{2}\right\} \tag{15}$$

$$\hat{N}_i(t) = \gamma_i^{-1}\int_0^t r_i\boldsymbol{e}_i^{\mathrm{T}}\dot{\boldsymbol{q}}_i\mathrm{d}\tau = \gamma_i^{-1}r_i\boldsymbol{e}_i^{\mathrm{T}}(\boldsymbol{q}_i(t) - \boldsymbol{q}_i(0)) \tag{16}$$

and γ_M and γ_i $(i = 1, 2)$ are appropriate positive constants and $\hat{M}(0)$ is an initial guess of the object mass M. The first term of the right hand side of Eq. (14) corresponds to direct compensation for the gravity term for the fingers, the second does to the damping for rotational moments of finger joints, the third to generation of an approximate opposing force, and the last two terms to estimates for the effect caused by the object weight and other unknown rotational moments affected at finger joints. More precisely, $\hat{N}_i$ plays a role of estimate for the unknown force

$$N_i = -\frac{Mg}{2}\cos(\theta + (-1)^i\theta_0) - \frac{f_d}{r_1 + r_2}\times\{l_w\sin\theta_0 - (-1)^i d\cos\theta_0\}, \qquad i = 1, 2 \tag{17}$$

where

$$\begin{cases} l_w = (l_1 + l_2 + r_1 + r_2)\cos\theta_0 + (Y_1 + Y_2)\sin\theta_0 \\ d = (Y_1 - Y_2)\cos\theta_0 - (l_1 + r_1 - l_2 - r_2)\sin\theta_0 \end{cases} \tag{18}$$

It is interesting to note that, in the case of objects with parallel surfaces (that is, $\theta_0 = 0$), N_i of Eq. (17) is reduced to the

https://doi.org/10.1017/S0263574707003840 Published online by Cambridge University Press

following simpler form:

$$N_i = -\frac{Mg}{2}\cos\theta + (-1)^i \frac{f_d}{r_1 + r_2}(Y_1 - Y_2), \qquad i = 1, 2 \tag{19}$$

Evidently from the definitions of estimates $\hat{M}$ and $\hat{N}_i$ ($i = 1, 2$) in Eqs. (15) and (16), control signals of Eq. (14) can be constructed easily in real-time calculation by referring to known kinematic parameters of the fingers and measurement data of finger-joint angles. It should be further emphasized that there is no need of any a-priori knowledge of kinematic parameters of the object such as location of its mass center, its width $l_1 + l_2$, weight M, and θ_0. In other words, the same control signals defined by Eq. (14) can be applied to grasping of an object either with parallel surfaces or with nonparallel surfaces without knowing *a priori* the shape of the object. Next, consider the problem how to withstand the gravitational force Mg of the object by using constraint forces f_i and λ_i ($i = 1, 2$) appearing in Eq. (11) or (13). In the case of objects with parallel surfaces, it is easy to see that if

$$\begin{cases} f_i = -(-1)^i \dfrac{Mg}{2}\sin\theta \\ \lambda_i = \dfrac{Mg}{2}\cos\theta \end{cases} \qquad i = 1, 2 \tag{20}$$

then the translational motion of Eq. (11) is reduced to

$$M\ddot{x} = 0, \qquad M\ddot{y} = 0 \tag{21}$$

In the case of an object with nonparallel surfaces as shown in Fig. 2, it is not easy but possible to have an insight in the balance of all four constraint forces f_i and λ_i ($i = 1, 2$) together with Mg and obtain the relation

$$\begin{cases} f_i = -(-1)^i \dfrac{Mg}{2}\sin(\theta + (-1)^i\theta_0) \\ \lambda_i = \dfrac{Mg}{2}\cos(\theta + (-1)^i\theta_0) \end{cases} \qquad i = 1, 2 \tag{22}$$

In fact, substitution of this equation into the first equation of Eq. (13) by referring Eqs. (T-5)–(T-8) in Table II leads to the same equation as Eq. (21).

Next, it is important to see that two quantities introduced in Eq. (18) have a physical meaning in relation to the following equality:

$$\begin{aligned} \|\boldsymbol{x}_{01} - \boldsymbol{x}_{02}\|^2 &= (x_{01} - x_{02})^2 + (y_{01} - y_{02})^2 \\ &= (l_w)^2 + d^2 \end{aligned} \tag{23}$$

This follows from the relations

$$\begin{cases} d = Y_1' - Y_2' - (r_1 - r_2)\sin\theta_0 \\ \quad = (x_{01} - x_{02})\sin\theta + (y_{01} - y_{02})\cos\theta \\ l_w = \tilde{l}\cos\theta_0 + (Y_1 + Y_2)\sin\theta_0 \\ \quad = -(x_{01} - x_{02})\cos\theta + (y_{01} - y_{02})\sin\theta \end{cases} \tag{24}$$

where

$$\begin{cases} Y_i' = Y_i\cos\theta_0 - l_i\sin\theta_0, & i = 1, 2 \\ \tilde{l} = l_1 + l_2 + r_1 + r_2 \end{cases} \tag{25}$$

and the constraint of Eq. (T-1) in Table I is employed in derivation of each of the last equalities in Eq. (24). In the case of objects with parallel surfaces, Eq. (23) is reduced to the simpler form:

$$\|\boldsymbol{x}_{01} - \boldsymbol{x}_{02}\|^2 = (Y_1 - Y_2)^2 + (\tilde{l})^2 \tag{26}$$

4. Closed-Loop Dynamics

Now, define

$$\begin{aligned} f_i &= \Delta f_i - (-1)^i \frac{Mg}{2}\sin(\theta + (-1)^i\theta_0) + \frac{f_d}{r_1 + r_2} \\ &\quad \times \{l_w\cos\theta_0 + (-1)^i d\sin\theta_0\}, \qquad i = 1, 2 \end{aligned} \tag{27}$$

$$\begin{aligned} \lambda_i &= \Delta\lambda_i + \frac{Mg}{2}\cos(\theta + (-1)^i\theta_0) + \frac{f_d}{r_1 + r_2} \\ &\quad \times \{l_w\sin\theta_0 - (-1)^i d\cos\theta_0\}, \qquad i = 1, 2 \end{aligned} \tag{28}$$

and note that from Eq. (24) it follows that

$$\begin{pmatrix} x_{01} - x_{02} \\ y_{01} - y_{02} \end{pmatrix} = R(\theta)\begin{pmatrix} -l_w \\ d \end{pmatrix} \tag{29}$$

where $R(\theta)$ denotes a 2-dimensional orthogonal matrix defined as

$$R(\theta) = \begin{pmatrix} \cos\theta & \sin\theta \\ -\sin\theta & \cos\theta \end{pmatrix} \tag{30}$$

and $f_0 = (1 + (r_1 + r_2)/(l_1 + l_2))f_d$. Then, from Eq. (29) and the expressions of $\partial Q_i/\partial \boldsymbol{q}_i$ and $\partial R_i/\partial \boldsymbol{q}_i$ given in Table II, it is possible to see that

$$\begin{aligned} &-\frac{f_d}{r_1 + r_2}\{l_w\cos\theta_0 + (-1)d\sin\theta_0\}\frac{\partial Q_i}{\partial \boldsymbol{q}_i} - \frac{f_d}{r_1 + r_2} \\ &\quad \times \{l_w\sin\theta_0 - (-1)^i d\cos\theta_0\}\frac{\partial R_i}{\partial \boldsymbol{q}_i} \\ &= (-1)^i \frac{f_d}{r_1 + r_2}\boldsymbol{J}_i^{\mathrm{T}}(\boldsymbol{q}_i)(\boldsymbol{x}_{01} - \boldsymbol{x}_{02}) + \frac{r_i f_d}{r_1 + r_2} \\ &\quad \times \{l_w\sin\theta_0 - (-1)^i d\cos\theta_0\}\boldsymbol{e}_i, \qquad i = 1, 2 \end{aligned} \tag{31}$$

By bearing this equality and the relation between Eq. (21) and (22) in mind, substituting the control signals $\boldsymbol{v}_i$ of Eq. (14) and Eqs. (27) and (28) into Eq. (12) yields the closed-loop

https://doi.org/10.1017/S0263574707003840 Published online by Cambridge University Press

dynamics:

$$H_i\ddot{\boldsymbol{q}}_i + \left(\frac{1}{2}\dot{H}_i + S_i\right)\dot{\boldsymbol{q}}_i + c_i\dot{\boldsymbol{q}}_i - \Delta f_i\frac{\partial Q_i}{\partial \boldsymbol{q}_i} - \Delta\lambda_i\frac{\partial R_i}{\partial \boldsymbol{q}_i} + \frac{\Delta M g}{2}\left(\frac{\partial y_{0i}}{\partial \boldsymbol{q}_i}\right) + r_i\Delta N_i\boldsymbol{e}_i = 0, \qquad i = 1, 2 \tag{32}$$

$$M\ddot{\boldsymbol{x}} - \sum_{i=1,2}\left(\Delta f_i\frac{\partial Q_i}{\partial \boldsymbol{x}} + \Delta\lambda_i\frac{\partial R_i}{\partial \boldsymbol{x}}\right) = 0 \tag{33}$$

$$I\ddot{\theta} - \sum_{i=1,2}\left(\Delta f_i\frac{\partial Q_i}{\partial \theta} + \Delta\lambda_i\frac{\partial R_i}{\partial \theta}\right) + S_N = 0 \tag{34}$$

where $\Delta M = \hat{M} - M$, $\Delta N_i = \hat{N}_i - N_i$, and S_N is defined as follows:

$$\begin{aligned} S_N &= \frac{f_d}{r_1 + r_2}[d\{(Y_1 + Y_2)\sin\theta_0 + (l_1 + l_2)\cos\theta_0\} \\ &\quad - l_w\{(Y_1 - Y_2)\cos\theta_0 - (l_1 - l_2)\sin\theta_0\}] - N \\ &= -f_d\left\{d\cos\theta_0 + \frac{r_1 - r_2}{r_1 + r_2}l_w\sin\theta_0\right\} - N \end{aligned} \tag{35}$$

$$\begin{aligned} N = \frac{Mg}{2}&\{Y_1\sin(\theta - \theta_0) + Y_2\sin(\theta + \theta_0) \\ &- l_1\cos(\theta - \theta_0) + l_2\cos(\theta + \theta_0)\} \end{aligned} \tag{36}$$

The last term of S_N in Eq. (35) has a special physical meaning. Since four algebraic constraints $Q_i = 0$ and $R_i = 0$ for $i = 1, 2$ (see Eqs. (T-1) and (T-3), given in Table I) can be expressed as

$$\begin{cases} R^{-1}(\theta - \theta_0)(\boldsymbol{x} - \boldsymbol{x}_{01}) = (l_1 + r_1, -Y_1)^{\mathrm{T}} \\ R^{-1}(\theta + \theta_0)(\boldsymbol{x} - \boldsymbol{x}_{02}) = -(l_2 + r_2, Y_2)^{\mathrm{T}} \end{cases} \tag{37}$$

from which it follows that

$$\begin{aligned} y - \frac{y_{01} + y_{02}}{2} = -\frac{1}{2}&[\{Y_1\cos(\theta - \theta_0) + Y_2\cos(\theta + \theta_0)\} \\ &+ \{(l_1 + r_1)\sin(\theta - \theta_0) \\ &- (l_2 + r_2)\sin(\theta + \theta_0)\}] \end{aligned} \tag{38}$$

it is possible to verify that

$$\frac{\partial\{Mg(y - (y_{01} + y_{02})/2)\}}{\partial\theta} = N \tag{39}$$

Note that the fourth term of $\boldsymbol{v}_i$ in Eq. (14) comes from the fact that the potential of the object $-Mgy$ under the gravity is approximated by the quantity $-\hat{M}g(y_{01} + y_{02})/2$. Thus, it is possible to see that taking inner products between $\dot{\boldsymbol{q}}_i$ and Eq. (32), $\dot{\boldsymbol{x}}$ and Eq. (33), and $\dot{\theta}$ and Eq. (34) yield the following relation:

$$\frac{\mathrm{d}}{\mathrm{d}t}E = -\sum_{i=1,2} c_i\|\dot{\boldsymbol{q}}\|^2 \tag{40}$$

where

$$\begin{aligned} E = K &+ \frac{\gamma_M}{2}\Delta M^2 + \frac{f_d}{2(r_1 + r_2)}(l_w^2 + d^2) \\ &+ \frac{1}{2}\{\gamma_1(\hat{N}_1)^2 + \gamma_2(\hat{N}_2)^2\} - Mg\Delta y \end{aligned} \tag{41}$$

$$\begin{aligned} \Delta y &= y - \frac{y_{01} + y_{02}}{2} \\ &= -\frac{1}{2}[\{Y_1\cos(\theta - \theta_0) + Y_2\cos(\theta + \theta_0)\} \\ &\quad + \{(l_1 + r_1)\sin(\theta - \theta_0) + (l_2 + r_2)\sin(\theta + \theta_0)\}] \end{aligned} \tag{42}$$

It should be noted again that

$$\frac{\partial Mg\Delta y}{\partial\theta} = N \tag{43}$$

and from Eqs. (24), (25), and (T-2) of Table I that

$$\begin{aligned} &\frac{\partial}{\partial\theta}\left\{\frac{f_d}{2(r_1 + r_2)}(l_w^2 + d^2)\right\} \\ &= \frac{f_d}{r_1 + r_2}\left(l_w\frac{\partial l_w}{\partial\theta} + d\frac{\partial d}{\partial\theta}\right) \\ &= -\frac{f_d}{r_1 + r_2}\{(r_1 + r_2)d\cos\theta_0 + (r_1 - r_2)l_w\sin\theta_0\} \\ &= S_N + N \end{aligned} \tag{44}$$

In a similar way, it follows that

$$\begin{aligned} &\frac{\partial}{\partial\boldsymbol{q}_i}\left\{\frac{f_d}{2(r_1 + r_2)}(l_w^2 + d^2) - Mg\Delta y\right\} \\ &= \frac{f_d}{r_1 + r_2}\left(l_w\frac{\partial l_w}{\partial\boldsymbol{q}_i} + d\frac{\partial d}{\partial\boldsymbol{q}_i} - Mg\frac{\partial\Delta y}{\partial\boldsymbol{q}_i}\right) \\ &= -r_i N_i\boldsymbol{e}_i \end{aligned} \tag{45}$$

Thus, it can be ascertained that applying Hamilton's principle for the Lagrangian

$$L = K - \tilde{P} + \sum_{i=1,2}(\Delta f_i Q_i + \Delta\lambda_i R_i) \tag{46}$$

where

$$\begin{aligned} \tilde{P} = \frac{1}{2}&\left\{\gamma_M\Delta M^2 + \frac{f_d}{r_1 + r_2}(l_w^2 + d^2) + \gamma_1\hat{N}_1^2 + \gamma_2\hat{N}_2^2\right\} \\ &- Mg\Delta y \end{aligned} \tag{47}$$

yields the Lagrange equation expressed by the set of Eqs. (32)–(34).

5. Simulation Results

Computer simulation of stable grasping for an object with nonparallel flat surfaces was carried out under the gravity effect by using Lagrange's equation of motion expressed by

https://doi.org/10.1017/S0263574707003840 Published online by Cambridge University Press

Table III. 3 d.o.f + 3 d.o.f physical parameters.

$m_{11} = m_{21}$	Link mass	0.045 [kg]
$m_{12} = m_{22}$	Link mass	0.025 [kg]
$m_{13} = m_{23}$	Link mass	0.015 [kg]
$I_{11} = I_{21}$	Inertia moment	1.584×10^{-5} [kg · m^2]
$I_{12} = I_{22}$	Inertia moment	3.169×10^{-6} [kg · m^2]
$I_{13} = I_{23}$	Inertia moment	8.450×10^{-7} [kg · m^2]
$l_{11} = l_{21}$	Link length	0.065 [m]
$l_{12} = l_{22}$	Link length	0.039 [m]
$l_{13} = l_{23}$	Link length	0.026 [m]
r_1	Radius	0.015 [m]
r_2	Radius	0.020 [m]
M	Object mass	0.040 [kg]
h	Object height	0.05000 [m]
I	Object inertia moment	1.26×10^{-5} [kg · m^2]
θ_0	Object inclination angle	$-15 \times \pi/180$ [rad]
l_1	Object length	0.012859 [m]
l_2	Object length	0.022390 [m]

Table IV. Parameters of control signals.

f_d	Internal force	2.0 [N]
$c_1 = c_2$	Damping coefficient	0.006 [msN]
γ_M	Regressor gain	0.01 [m^2/kgs^2]
γ_1	Regressor gain	0.001 [s^2/kg]
γ_2	Regressor gain	0.001 [s^2/kg]

Table V. Initial values of simulation.

$Y_1(0)$	Internal value of $Y_1(t)$	0.001 [m]
$Y_2(0)$	Internal value of $Y_2(t)$	0.000 [m]
$\hat{M}(0)$	Internal value of $\hat{M}(t)$	0.010 [kg]
$\hat{N}_1(0)$	Internal value of $\hat{N}_1(t)$	0.000 [N]
$\hat{N}_2(0)$	Internal value of $\hat{N}_2(t)$	0.000 [N]

Eqs. (12) and (13) and feeding the control signals $\boldsymbol{v}_i$ $(i = 1, 2)$ of Eq. (14). In order to incorporate the holonomic constraints of (T-1) and (T-2) described in Table I[10], the so-called constraint stabilization method (CSM) was used. All physical parameters necessary for conducting the simulation are given in Table III, parameters and gains necessary for determining the control signals are summarized in Table IV, and initial values for estimates are presented in Table V. Figure 3 shows that the first two physical variables $Y_1' - Y_2'$ and θ converge asymptotically to their corresponding constants within 1s while constraint forces Δf_i and $\Delta\lambda_i$ $(i = 1, 2)$, other variables ΔN_i $(i = 1, 2)$ and S_N, and the object mass estimation error ΔM converge to zero quickly within 1s, too. As it will be discussed in the next section and Appendix A, the speed of convergence of all such physical variables to their corresponding constants is exponential in the independent variable of time t. It should also be important to remark that the estimate $\hat{M}(t)$ of the object mass tends to its true value M eventually as $t \to \infty$ due to the redundancy of finger joints. In fact, in the case of a pair of fingers with two joints, $\hat{M}(t)$ converges to some constant M_∞ as $t \to \infty$ but M_∞ does not necessarily coincide with the true value M, as shown in Fig. 4. Figure 4 shows transient responses of physical variables in the case of a pair of robot fingers with two joints and an object with parallel flat surfaces. In this case, all physical parameters

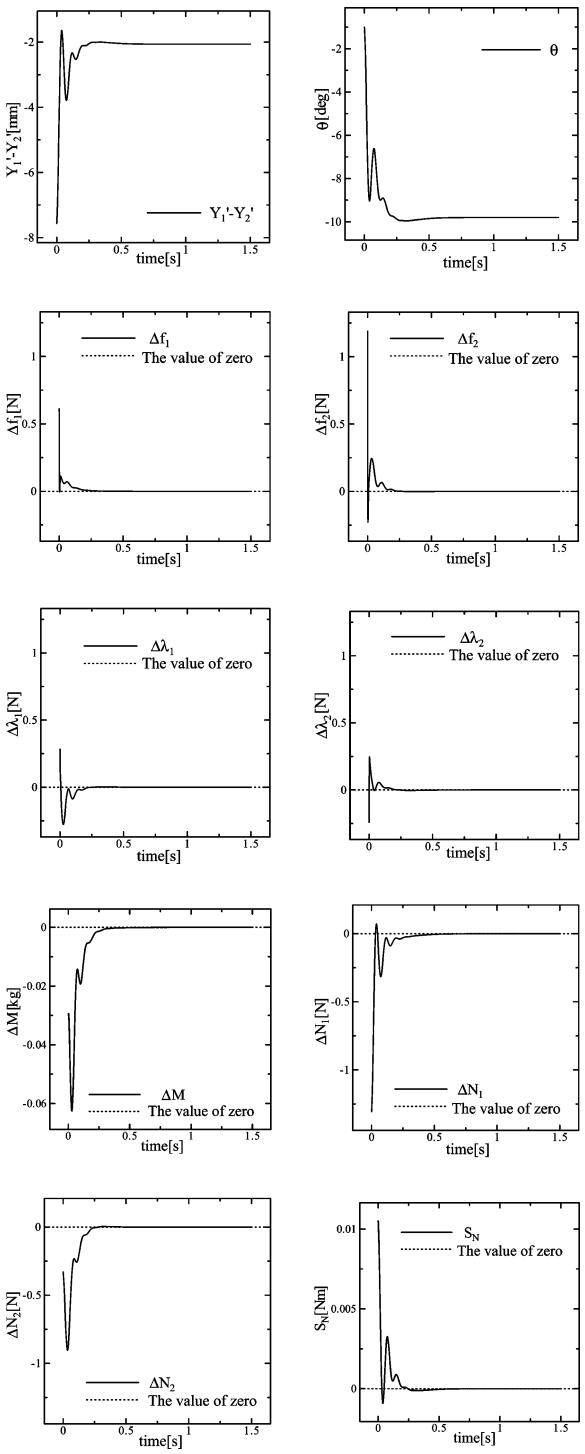


Fig. 3. Transient responses of physical variables in the case of a pair of fingers with three joints.

of the setup of the pair of fingers and object are summarized in Table VI and control gains and initial positions are given in Tables VII and VIII, respectively. It is interesting to note, as predicted theoretically in the next section, that all physical variables Δf_i, $\Delta\lambda_i$, ΔN_i $(i = 1, 2)$, S_N, and ΔM converge to constants that may not necessarily be zero. It should also be remarked that, as seen from both Figs. 3 and 4, $f_i(t)$ $(i = 1, 2)$ are maintained to be positive, which implies that the condition of rigid contacts between finger-ends and object surfaces does not break down during motion of the fingers

https://doi.org/10.1017/S0263574707003840 Published online by Cambridge University Press

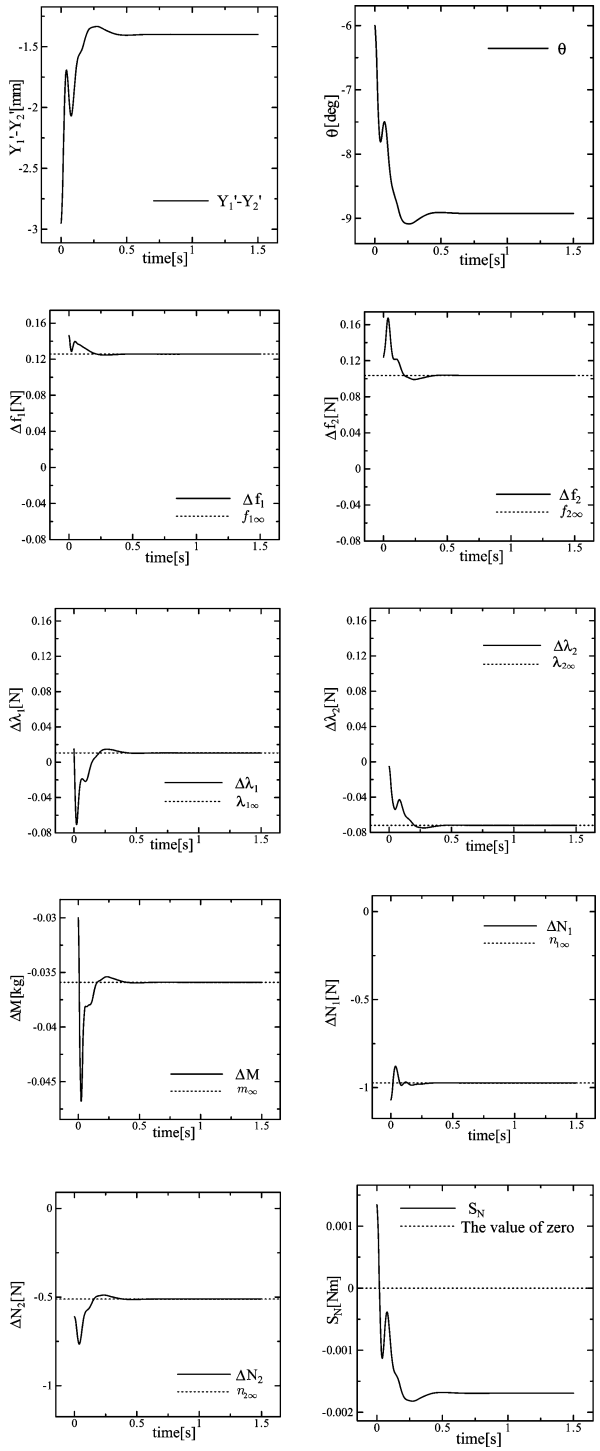


Fig. 4. Transient responses of physical variables in the case of a pair of two-DOF fingers and the object with parallel surfaces.

and object. Finally, it should be emphasized again that the control signal used in this simulation does not include any prior knowledge of the object such as nonuniformness of the mass density of the object (i.e., $l_1 \neq l_2$), nonparallelness of its side surfaces ($\theta_0 \neq 0$), and object masses M and inertia I.

Even if $\theta_0 > 0$, the stability analysis does not incur a problem as far as the rolling contacts are maintained without slipping. However, in practical situations, since the direction of a net force at a contact point consisting of the pressing force f_1 normal to the object surface plus the effective gravity force with magnitude $(Mg/2)\cos\theta_0$ tangent to the surface protrudes out of the friction cone as seen in Fig. 5, it is difficult to prevent the object from slipping if θ_0 is relatively large around $\theta_0 = 15^\circ$.

Table VI. 2 d.o.f + 2 d.o.f physical parameters.

$m_{11} = m_{21}$	Link mass	0.0451 [kg]
$m_{12} = m_{22}$	Link mass	0.0252 [kg]
$I_{11} = I_{21}$	Inertia moment	2.53×10^{-5} [kg · m^2]
$I_{12} = I_{22}$	Inertia moment	7.94×10^{-6} [kg · m^2]
$l_{11} = l_{21}$	Link length	0.082 [m]
$l_{12} = l_{22}$	Link length	0.0615 [m]
r_1	Radius	0.015 [m]
r_2	Radius	0.020 [m]
M	Object mass	0.040 [kg]
h	Object height	0.05000 [m]
I	Object inertia moment	1.26×10^{-5} [kg · m^2]
θ_0	Object inclination angle	$-15 \times \pi/180$ [rad]
l_1	Object length	0.012859 [m]
l_2	Object length	0.022390 [m]

Table VII. Parameters of control signals.

f_d	Internal force	2.0 [N]
$c_1 = c_2$	Damping coefficient	0.006 [msN]
γ_M	Regressor gain	0.01 [m^2/kgs^2]
γ_1	Regressor gain	0.001 [s^2/kg]
γ_2	Regressor gain	0.001 [s^2/kg]

Table VIII. Initial values of Simulation.

$Y_1(0)$	Internal value of $Y_1(t)$	−0.0035 [m]
$Y_2(0)$	Internal value of $Y_2(t)$	−0.003 [m]
$\hat{M}(0)$	Internal value of $\hat{M}(t)$	0.010 [kg]
$\hat{N}_1(0)$	Internal value of $\hat{N}_1(t)$	0.000 [N]
$\hat{N}_2(0)$	Internal value of $\hat{N}_2(t)$	0.000 [N]

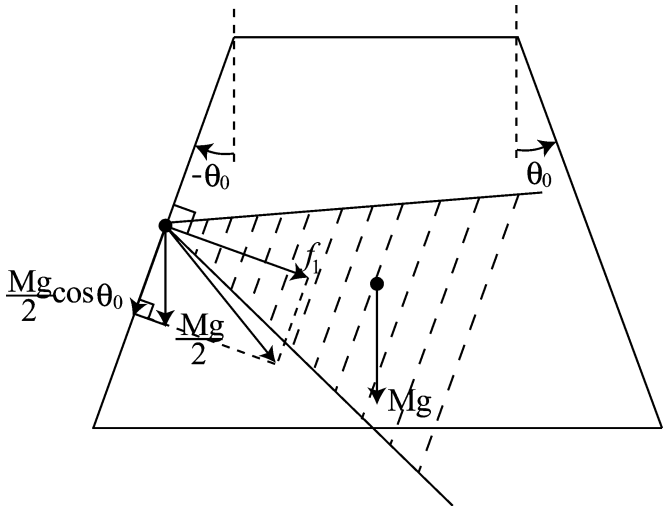


Fig. 5. The direction of a net force of f_1 normal to the object surface plus gravity force $(Mg/2)\cos\theta_0$ affected along the surface is inclined to protrude beyond the friction cone.

https://doi.org/10.1017/S0263574707003840 Published online by Cambridge University Press

6. Proof of Convergence to Force/Torque Balance

Now we are in a position to discuss the problem of stability of an equilibrium still state satisfying the force/torque balance in a dynamic sense. At the same time, it is important to prove convergence of the trajectory of any solution to the closed-loop dynamics of Eqs. (32), (33), and (34) starting from a neighborhood of the reference equilibrium state with force/torque balance.

Firstly, note that, in the case of a pair of robot fingers depicted in Fig. 2, the trajectory of any solution to the closed-loop dynamics of Eqs. (32)–(34) should lie on the 10-dimensional manifold in the state space R^{18} as defined by

$$M_{10} = \{(\boldsymbol{q}_1, \boldsymbol{q}_2, \boldsymbol{x}, \theta, \dot{\boldsymbol{q}}_1, \dot{\boldsymbol{q}}_2, \dot{\boldsymbol{x}}, \dot{\theta}) : Q_i = 0 \quad R_i = 0, \dot{Q}_i = 0, \dot{R}_i = 0 \qquad (i = 1, 2)\}$$

Since the condition of force/torque balance for the 2D object is described by the equation of a linear form of four 2D wrench vectors

$$\boldsymbol{w}_{fi} = \left(\frac{\partial Q_i}{\partial x}, \frac{\partial Q_i}{\partial y}, \frac{\partial Q_i}{\partial \theta}\right)^{\mathrm{T}},$$
$$\boldsymbol{w}_{\lambda i} = \left(\frac{\partial R_i}{\partial x}, \frac{\partial R_i}{\partial y}, \frac{\partial R_i}{\partial \theta}\right)^{\mathrm{T}}, \qquad i = 1, 2 \tag{48}$$

as

$$\sum_{i=1,2} (\Delta f_i \boldsymbol{w}_{fi} + \Delta\lambda_i \boldsymbol{w}_{\lambda i}) - (0, 0, S_N)^{\mathrm{T}} = 0 \tag{49}$$

any equilibrium still state of force–torque balance should belong to the 2-dimensional manifold defined as

$$EM_2 = \{(\boldsymbol{q}_1, \boldsymbol{q}_2, \boldsymbol{x}, \theta, \dot{\boldsymbol{q}}_1 = 0, \dot{\boldsymbol{q}}_2 = 0, \dot{\boldsymbol{x}} = 0, \dot{\theta} = 0) : \quad Q_i = 0, R_i = 0 \qquad (i = 1, 2) \quad \text{and} \quad \text{Eq. (49)}\}$$

This is called the equilibrium-point (EP) manifold in this paper and can be regarded as the 2D manifold embedded in the 9-dimensional configuration space defined as $R^9 = \{(\boldsymbol{q}_1, \boldsymbol{q}_2, \boldsymbol{x}, \theta)\}$.

Secondly, consider an arbitrary initial state $(z(0), \dot{z}(0))$ where $z = (\boldsymbol{q}_1^{\mathrm{T}}, \boldsymbol{q}_2^{\mathrm{T}}, r^{-1}\boldsymbol{x}, \theta)^{\mathrm{T}}$ and r is a scale factor introduced for balancing the magnitudes of all eigenvalues of inertia matrices $H_i(\boldsymbol{q}_i)$ and the inertia moment I of the object with the scaled magnitude r^2M of object mass M. We assume that there is an equilibrium pose z^0 belonging to EM_2 and consider a neighborhood of z^0 with $\delta > 0$ in the state space such that

$$|E(z(0), \dot{z}(0)) - E(z^0, \dot{z} = 0)| \le \delta \tag{50}$$

where

$$E(z, \dot{z}) = K(z, \dot{z}) + \tilde{P}(z) \tag{51}$$

and K stands for the total kinetic energy and $\tilde{P}$ stands for the artificial potential defined by Eq. (47).

Thirdly, we verify that the artificial potential function $\tilde{P}$ has a minimum value at some still state $z = z_\infty$ under the constraints $Q_i = 0$ and $R_i = 0$ for $i = 1, 2$. To do this, note that, according to Eq. (45) and definitions of $\hat{M}$ and $\hat{N}_i$ in Eqs. (15) and (16), we can obtain

$$\frac{\partial \tilde{P}}{\partial \boldsymbol{q}_i} = \frac{\Delta M g}{2}\left(\frac{\partial y_{0i}}{\partial \boldsymbol{q}_i}\right) + r_i \Delta N_i \boldsymbol{e}_i \tag{52}$$

which is equivalent to the sum of last two terms in the left hand side of Eq. (32). Further, note that, according to Eqs. (43) and (44), we obtain

$$\frac{\partial \tilde{P}}{\partial \theta} = S_N \tag{53}$$

which is equivalent to the last term in the left hand side of Eq. (34). Next, it is convenient to remark that, except the term $(\gamma_M/2)\Delta M^2$, other terms of $\tilde{P}$ is a function of θ and p_i $(i = 1, 2)$ which are defined as

$$p_i = \sum_{j=1}^{3} q_{ij} \tag{54}$$

Hence, define

$$\begin{aligned} P_0 &= \tilde{P} - (\gamma_M/2)\Delta M^2 \\ &= \frac{f_d}{2(r_1 + r_2)}\left(l_w^2 + d^2\right) - Mg\Delta y \\ &\quad + \frac{1}{2}\left\{\gamma_1 \hat{N}_1^2 + \gamma_2 \hat{N}_2^2\right\} \end{aligned} \tag{55}$$

Then, it is easy to see that

$$\begin{cases} \partial P_0/\partial\theta = S_N \\ \partial P_0/\partial p_i = r_i(\hat{N}_i - N_i) = r_i \Delta N_i \end{cases} \tag{56}$$

Further, the Hessian matrix of P_0 in p_1, p_2, and θ can be obtained in the following way:

$$\begin{aligned} \frac{\partial^2 P_0}{\partial \theta^2} &= f_d\left\{(r_1 + r_2)\cos^2\theta_0 + \frac{(r_1 - r_2)^2}{r_1 + r_2}\sin^2\theta_0\right\} \\ &\quad - \frac{Mg}{2}\{Y_1\cos(\theta - \theta_0) + Y_2\cos(\theta + \theta_0) \\ &\quad + (l_1 - r_1)\sin(\theta - \theta_0) - (l_2 - r_2)\sin(\theta + \theta_0)\} \end{aligned} \tag{57a}$$

$$\begin{aligned} \frac{\partial^2 P_0}{\partial\theta\partial p_i} &= \frac{r_i f_d}{r_1 + r_2}\{(-1)^i(r_1 + r_2)\cos^2\theta_0 - (r_1 - r_2)\sin^2\theta_0\} \\ &\quad - \frac{Mg}{2} r_i \sin(\theta + (-1)^i\theta_0), \quad i = 1, 2 \end{aligned} \tag{57b}$$

$$\frac{\partial^2 P_0}{\partial p_2 \partial p_1} = \frac{\partial^2 P_0}{\partial p_1 \partial p_2} = \frac{r_1 r_2 f_d}{r_1 + r_2}(\sin^2\theta_0 - \cos^2\theta_0) \tag{57c}$$

$$\frac{\partial^2 P_0}{\partial p_i^2} = r_i^2\left(\frac{1}{\gamma_i} + \frac{f_d}{r_1 + r_2}\right), \qquad i = 1, 2 \tag{57d}$$

If f_d is considerably larger than Mg and γ_i $(i = 1, 2)$ are selected sufficiently small in comparison with $(r_1 + r_2)/f_d$,

https://doi.org/10.1017/S0263574707003840 Published online by Cambridge University Press

then this Hessian matrix becomes positive definite in the specified neighborhood of $z^0 \in EM_2$. Thus, we denote the minimum of P_0 by $P_{0\infty}$ and assume that $P_0 = P_{0\infty}$ is attained at $p_i = p_{i\infty}$ $(i = 1, 2)$ and $\theta = \theta_\infty$. Then, $\bar{E} = E - P_{0\infty}$ becomes positive definite in the neighborhood of z^0 and satisfies

$$\frac{\mathrm{d}}{\mathrm{d}t}\bar{E} = \sum_{i=1,2} -c_i \|\dot{\boldsymbol{q}}_i\|^2 \tag{58}$$

according to Eq. (40). This means that

$$\int_0^\infty \|\dot{\boldsymbol{q}}_i(t)\|^2 \mathrm{d}t < c_i^{-1}\bar{E}(0) \tag{59}$$

and, by referring to lemma $C1$ of Appendix C,[11] $\dot{\boldsymbol{q}}_i(t) \to 0$ as $t \to \infty$. Further, $\dot{\boldsymbol{x}}(t) \to 0$ and $\dot{\theta}(t) \to 0$ as $t \to \infty$ due to the holonomic constraints $\dot{Q}_i = 0$ and $\dot{R}_i = 0$ $(i = 1, 2)$ as already discussed in the previous papers.[4,5] Thus, $\dot{\boldsymbol{z}}(t) \to 0$ as $t \to \infty$ and this in turn implies $\boldsymbol{z}(t) \to 0$ as $t \to \infty$ (see lemma $C3$ of Appendix C[11]). Hence, it follows from Eqs. (32)–(34) that

$$-[A, B]\Delta\boldsymbol{\lambda} + \boldsymbol{d}_N \to 0 \quad \text{as} \quad t \to \infty \tag{60}$$

where

$$A = \begin{pmatrix} \dfrac{\partial Q_1}{\partial \boldsymbol{q}_1} & 0_3 & \dfrac{\partial R_1}{\partial \boldsymbol{q}_1} & 0_3 \\ 0_3 & \dfrac{\partial Q_2}{\partial \boldsymbol{q}_2} & 0_3 & \dfrac{\partial R_2}{\partial \boldsymbol{q}_2} \\ \dfrac{\partial Q_1}{\partial \bar{\boldsymbol{x}}} & \dfrac{\partial Q_2}{\partial \bar{\boldsymbol{x}}} & \dfrac{\partial R_1}{\partial \bar{\boldsymbol{x}}} & \dfrac{\partial R_2}{\partial \bar{\boldsymbol{x}}} \\ \dfrac{\partial Q_1}{\partial \theta} & \dfrac{\partial Q_2}{\partial \theta} & \dfrac{\partial R_1}{\partial \theta} & \dfrac{\partial R_2}{\partial \theta} \end{pmatrix} \tag{61}$$

$$B = \begin{pmatrix} -\dfrac{\partial y_{01}}{\partial \boldsymbol{q}_1} & -r_1\boldsymbol{e}_1 & 0_3 \\ -\dfrac{\partial y_{02}}{\partial \boldsymbol{q}_2} & 0_3 & -r_2\boldsymbol{e}_2 \\ 0_2 & 0_2 & 0_2 \\ 0 & 0 & 0 \end{pmatrix} \tag{62}$$

$$\Delta\boldsymbol{\lambda} = (\Delta f_1, \Delta f_2, \Delta\lambda_1, \Delta\lambda_2, \Delta Mg/2, \Delta N_1, \Delta N_2)^{\mathrm{T}} \tag{63}$$

$$\boldsymbol{d}_N = (0, \ldots, 0, S_N), \tag{64}$$

and $\bar{\boldsymbol{x}} = r^{-1}\boldsymbol{x}$. Note that $\Delta\boldsymbol{\lambda}$ is of 7-dimensional vector, $[A, B]$ is of 9×7 matrix, d_N is of 9-dimension. It is also important to note that $[A, B]$ is of full rank (i.e., $\mathrm{rank}([A, B]) = 7$) in the neighborhood of z^0. Therefore, Eq. (60) means that

$$\Delta\boldsymbol{\lambda}(t) \to 0 \quad \text{and} \quad S_N(t) \to 0 \quad \text{as} \quad t \to \infty \tag{65}$$

This in turn implies that as $t \to \infty$ the equality (49) is achieved. In other words, the solution $\boldsymbol{z}(t)$ to the closed-loop dynamics expressed by Eqs. (32)–(34) starting from an arbitrary state $\boldsymbol{z}(0)$ in a neighborhood of z^0 converges to an equilibrium still state as $t \to \infty$, that belongs to EM_2 and satisfies the force/torque balance. Furthermore, as predicted from the previous works,[3,4] it is possible to confirm that not only physical variables p_i $(i = 1, 2)$, θ, ΔM but also all velocity variables $\dot{\boldsymbol{z}}(t)$ and position variables $\boldsymbol{z}(t)$ converges exponentially to their corresponding constants as $t \to \infty$, that is, $\|\dot{\boldsymbol{z}}(t)\| \to 0$ and $\|\boldsymbol{z}(t) - \boldsymbol{z}_\infty\| \to 0$ exponentially as $t \to \infty$ for some $\boldsymbol{z}_\infty$. The details of the proof is presented in Appendix.

In the case that one of the fingers has two joints and another has three joints, a similar result to the above can be obtained. However, in the case that each robot finger has two joints as shown in Fig. 1, the situation of convergence of solution trajectories differs from the case of robot fingers with redundant joints. In this case, the position state vector $\boldsymbol{z}$ is of 7-dimensional and $[A, B]$ is of 7×7-matrix, that is, it becomes a square matrix. Notwithstanding this fact, the lemma $C1$ of Appendix[11] can be applied in an analogous way as discussed in the paragraph after Eq. (59). Then, Eq. (60) should be regarded as

$$A \to A_\infty, \quad B \to B_\infty, \quad \Delta\boldsymbol{\lambda} \to \boldsymbol{\lambda}_\infty, \quad \text{and} \quad \boldsymbol{d}_N \to \boldsymbol{d}_\infty \tag{66}$$

as $t \to \infty$ so that

$$[A_\infty, B_\infty]\boldsymbol{\lambda}_\infty = \boldsymbol{d}_\infty \tag{67}$$

where A_∞ and B_∞ a constant matrix, $\boldsymbol{\lambda}_\infty$ and $\boldsymbol{d}_\infty$ are a constant vector. Furthermore, even in this case, it is possible to show that the speed of asymptotic convergence of $\dot{\boldsymbol{z}} \to 0$, $\boldsymbol{z} \to \boldsymbol{z}_\infty$, and $\Delta\boldsymbol{\lambda} \to \boldsymbol{\lambda}_\infty$ is exponential in t. The proof is inferable from Appendix, and therefore is omitted in this paper.

7. Conclusions

This paper shows theoretically and through numerical simulations that stable precision prehension of a rigid object by a pair of multijoint robot fingers with hemispherical ends can be established in a blind manner under the effect of gravity. It is assumed that motion of the overall fingers–object system is confined to a vertical plane. As a byproduct of the theory it is shown that at least the total of four joints for the pair of fingers (for example, thumb with 2 DOF and index finger with 2 DOF) is necessary and sufficient for realizing stable grasping satisfying the force/torque balance. However, in order that an estimator of unknown object mass converges asymptotically to its true value, at least a total of five finger joints are required. Some experimental results have been presented in a separate paper.[12]

The method presented in this paper for proving stability and convergence of solutions to the closed-loop dynamics of the overall fingers–object system can be extended to cope with 3-dimensional object grasping and manipulation under the gravity effect and nonholonomic constraints. At present, it has been shown that a similar control signal to that given in Eq. (14) can work well even in the case of 3D object grasping.[13,14] However, only the case of rigid object with parallel flat surfaces is tackled in a rigorous mathematical way.[14]

https://doi.org/10.1017/S0263574707003840 Published online by Cambridge University Press

References

1. A. Bicchi, "Hands for dexterous manipulation and robust grasping: A difficult road toward simplicity," *IEEE Trans. Rob. Autom.* **16**(6), 652–662 (2000).
2. R. M. Murray, Z. Li, and S. S. Sastry, *A Mathematical Introduction to Robotic Manipulation* (CRC Press. Boca Raton, FL. USA and Tokyo. Japan, 1994).
3. S. Arimoto, K. Tahara, J.-H. Bae, and M. Yoshida, "A stability theory on a manifold: Concurrent realization of grasp and orientation control of an object by a pair of robot fingers," *Robotica* **21**(2), 163–178 (2003).
4. S. Arimoto, M. Yoshida, J.-H. Bae, and K. Tahara, "Dynamic force/torque balance of 2D polygonal objects by a pair of rolling contacts and sensory-motor coordination," *J. Robot. Syst.* **20**(9), 517–537 (2003).
5. S. Arimoto, "Intelligent control of multi-fingered hands," *Annu. Rev. Control* **28**(1), 75–85 (2004).
6. S. Arimoto, J.-H. Bae, H. Hashiguchi, and R. Ozawa, "Natural resolution of ill-posedness of inverse kinematics for redundant robots under constraints," *Comm. Inf. Syst.* **4**(1), 1–28 (2004).
7. R. Ozawa, S. Arimoto, M. Yoshida, and S. Nakamura, "Stable grasping and relative angle control of an object by dual finger robots without object sensing," *Proceedings of the 2004 IEEE International Conference on Robotics and Automation*, New Orleans, LA, USA (Apr. 26–May 1, 2004) pp. 1694–1699.
8. M. L. Latash, *Neurophysiological Basis of Movement* (Human Kinetics, Champaign, IL. USA, 1998).
9. C. L. Mackenzie and T. Iberall, *The Grasping Hand, Advances In Psychology 104* (Elsevier Science Ltd. New York, NY. USA, 1994).
10. J. Baumgarte, "Stabilization of constraints and integrals of motion in dynamical systems," *Comput. Meth. Appl. Mech. Eng.* **1**(1), 1–16 (1972).
11. S. Arimoto, *Control Theory of Non-Linear Mechanical Systems: A Passivity-Based and Circuit-Theoretic Approach* (Oxford Univ Press, Oxford, UK, 1996).
12. S. Arimoto, M. Yoshida, and R. Ozawa, "Pinching without object information under the gravity effect," *Proceedings of the 22nd Annual Conference of the RSJ (in Japanese)*, Gifu, Japan (Sept. 15–17, 2004) 2J13.
13. S. Arimoto, M. Yoshida, and J.-H. Bae, "Stable "blind grasping" of a 3-D object under non-holonomic constraints," *Proceedings of the 2006 IEEE International Conference on Robotics and Automation*, Orlando, Florida, USA. (May 15–19, 2006) pp. 2124–2130.
14. S. Arimoto, M. Yoshida, and J.-H. Bae, "Modeling of 3-D object manipulation by multi-joint robot fingers under non-holonomic constraints and stable blind grasping", *in a special issue on ACMD' 06, JSME J. of System Design and Dynamics* **1**(3), (to be published) 2007.
15. S. Arimoto, M. Yoshida, J.-H. Bae, "Stability of 3D-object grasping under non-holonomic constraints and the gravity," *Proceedings of 8th International IFAC Symposium on Robot Control*, Bologna, Italy (Sept. 6–8, 2006) R-046.

Appendix

First it is convenient to rewrite the closed-loop dynamics of Eqs. (32)–(34) in the following vector–matrix form:

$$H\ddot{z} + \left(\frac{1}{2}\dot{H} + S\right)\dot{z} + C\dot{z} - [A,\, B]\Delta\boldsymbol{\lambda} + \boldsymbol{d}_N = 0 \qquad \text{(A-1)}$$

where $\boldsymbol{z} = (\boldsymbol{q}_1^{\mathrm{T}}, \boldsymbol{q}_2^{\mathrm{T}}, r^{-1}\boldsymbol{x}^{\mathrm{T}}, \theta)^{\mathrm{T}}$ and

$$\begin{cases} H = \mathrm{diag}(H_1,\, H_2,\, r^2 M I_2,\, I) \\ S = \mathrm{diag}(S_1,\, S_2,\, 0_2,\, 0) \\ C = \mathrm{diag}(c_1 I_3,\, c_2 I_3,\, 0_2,\, 0) \end{cases} \qquad \text{(A-2)}$$

and I_3 denotes the 3×3 identity matrix and 0_2 the 2×2 zero matrix. Second we denote the Hessian matrix of P_0 in p_1, p_2, and θ by G whose entries are given in Eqs. (57a)–(57d). Then, the scalar function $\tilde{P}$ defined in Eq. (47) can be approximated as

$$\tilde{P} = \frac{\gamma_M}{2}\Delta M^2 + \frac{1}{2}(\boldsymbol{p} - \boldsymbol{p}_\infty)^{\mathrm{T}} G(\boldsymbol{p} - \boldsymbol{p}_\infty) + P_{0\infty} + O(\|\Delta\boldsymbol{p}\|^3) \qquad \text{(A-3)}$$

where $\boldsymbol{p} = (p_1,\, p_2,\, p_3)$, $p_3 = \theta$, and $\boldsymbol{p}_\infty$ denotes the vector which $\boldsymbol{p}$ converges to as $t \to \infty$, $P_{0\infty}$ denotes the minimum value of P_0 (or the constant that P_0 converges to as $t \to \infty$), $\Delta\boldsymbol{p} = \boldsymbol{p} - \boldsymbol{p}_\infty$, and $O(\|\Delta\boldsymbol{p}\|^3)$ stands for a remaining higher term in $\Delta\boldsymbol{p}$. Thirdly, we define the following four vectors:

$$\begin{cases} \bar{\boldsymbol{e}}_1 = \begin{pmatrix} r_1\boldsymbol{e}_1 \\ 0_3 \\ 0_3 \end{pmatrix},\ \bar{\boldsymbol{e}}_2 = \begin{pmatrix} 0_3 \\ r_2\boldsymbol{e}_2 \\ 0_3 \end{pmatrix}, \\ \bar{\boldsymbol{e}}_3 = \begin{pmatrix} 0_3 \\ 0_5 \\ r_3 \end{pmatrix},\ \bar{\boldsymbol{e}}_M = \begin{pmatrix} \partial y_{01}/\partial \boldsymbol{q}_1 \\ \partial y_{02}/\partial \boldsymbol{q}_2 \\ 0_3 \end{pmatrix} \end{cases} \qquad \text{(A-4)}$$

Note that, by definitions of $\boldsymbol{d}_N$ (Eq. (64)) and B (Eq. (62)), it follows that

$$\begin{aligned} &-B\Delta\boldsymbol{m} + \boldsymbol{d}_N \\ &= \frac{\Delta M g}{2}\bar{\boldsymbol{e}}_M + \Delta N_1\bar{\boldsymbol{e}}_1 + \Delta N_2\bar{\boldsymbol{e}}_2 + r_3^{-1}S_N\bar{\boldsymbol{e}}_3 \\ &= [-B,\, \bar{\boldsymbol{e}}_3]\left[\Delta\boldsymbol{m}^{\mathrm{T}},\, r_3^{-1}S_N\right]^{\mathrm{T}} \end{aligned} \qquad \text{(A-5)}$$

where $\Delta\boldsymbol{m} = (\Delta M g/2,\, \Delta N_1,\, \Delta N_2)^{\mathrm{T}}$. Fourth, introduce the following four 9×7 matrices:

$$\begin{cases} A_M^{\mathrm{T}} = (A,\, \bar{\boldsymbol{e}}_1,\, \bar{\boldsymbol{e}}_2,\, \bar{\boldsymbol{e}}_3),\ A_1^{\mathrm{T}} = (A,\, \bar{\boldsymbol{e}}_M,\, \bar{\boldsymbol{e}}_2,\, \bar{\boldsymbol{e}}_3) \\ A_2^{\mathrm{T}} = (A,\, \bar{\boldsymbol{e}}_M,\, \bar{\boldsymbol{e}}_1,\, \bar{\boldsymbol{e}}_3),\ A_3^{\mathrm{T}} = (A,\, \bar{\boldsymbol{e}}_M,\, \bar{\boldsymbol{e}}_1,\, \bar{\boldsymbol{e}}_2) \end{cases} \qquad \text{(A-6)}$$

and define the following four projection matrices

$$\begin{cases} P_M = (I_9 - A_M^+ A_M),\ P_1 = (I_9 - A_1^+ A_1) \\ P_2 = (I_9 - A_2^+ A_2),\ P_3 = (I_9 - A_3^+ A_3) \end{cases} \qquad \text{(A-7)}$$

where A_M^+ denotes the pseudo-inverse of 7×9 matrix A_M, and A_i^+ that of A_i for $i = 1, 2, 3$. Note that

$$P_\xi A = 0, \quad P_\eta\bar{\boldsymbol{e}}_\xi = 0\ (\xi \neq \eta) \qquad \text{(A-8)}$$

where ξ, η denote one of symbols 1, 2, 3 and M. Fifthly, let us introduce the following 9-dimensional vector:

$$\boldsymbol{w} = \left(P_M\bar{\boldsymbol{e}}_M\frac{\sqrt{\gamma_M}}{\|\bar{\boldsymbol{e}}_M\|^2}\right)\Delta M + \sum_{i=1}^{3} P_i\bar{\boldsymbol{e}}_i\frac{\Delta p_i}{\|\bar{\boldsymbol{e}}_i\|^2} \qquad \text{(A-9)}$$

Then, consider a scalar quantity

$$V = \dot{\boldsymbol{z}}^{\mathrm{T}} H\boldsymbol{w} \qquad \text{(A-10)}$$

https://doi.org/10.1017/S0263574707003840 Published online by Cambridge University Press

and notice that every positive eigenvalue of the overall inertia matrix H is at most of order $O(10^{-5})$ and each diagonal entry of the Hessian matrix G is positive and at least of $O(10^{-1})$. Since it follows that

$$\left|\dot{z}^{\mathrm{T}} H P_M \bar{e}_M \frac{\sqrt{\gamma_M}}{\|\bar{e}_M\|^2}\Delta M\right| \leq \frac{\dot{z}^{\mathrm{T}} H H \dot{z}}{\|\bar{e}_M\|^2} + \frac{\bar{e}_M^{\mathrm{T}} P_M \bar{e}_M}{4\|\bar{e}_M\|^2}\gamma_M \Delta M^2 \leq \frac{\dot{z}^{\mathrm{T}} H H \dot{z}}{\|\bar{e}_M\|^2} + \frac{\gamma_M}{4}\Delta M^2 \tag{A-11}$$

$$\left|\dot{z}^{\mathrm{T}} H P_i \bar{e}_i \frac{\Delta p_i}{\|\bar{e}_i\|^2}\right| \leq \frac{(3/2)}{g_{ii}\|\bar{e}_i\|^2}\dot{z}^{\mathrm{T}} H H \dot{z} + \frac{g_{ii}}{6}\Delta p_i^2 \tag{A-12}$$

the absolute value of the scalar quantity V can be bounded as follows:

$$|V| \leq \left(\frac{1}{\|\bar{e}_M\|^2} + \sum_{i=1}^{3}\frac{3/2}{g_{ii}\|\bar{e}_i\|^2}\right)\dot{z}^{\mathrm{T}} H H \dot{z} + \frac{1}{3}\left(\frac{3}{4}\gamma_M \Delta M^2 + \sum_{i=1}^{3}\frac{1}{2}g_{ii}\Delta p_i^2\right) \tag{A-13}$$

The diagonal part $G_D = \mathrm{diag}(g_{ii})$ of the matrix $G = (g_{ij})$ is dominant in G and reasonably assumed to satisfy

$$\frac{1}{2}\Delta p^{\mathrm{T}} G_D \Delta \boldsymbol{p} \leq \frac{3}{4}(P_0 - P_{0\infty}) \tag{A-14}$$

Thus, it follows from Eqs. (A-13) and (A-14) that

$$|V| \leq \frac{1}{2}(K + \tilde{P} - P_{0\infty}) \tag{A-15}$$

in which the first term of the right hand side of Eq. (A-13) is bounded by the quantity $(1/2)K$ since the maximum eigenvalue of matrix H is of $O(10^{-5})$ and far smaller than $\|\bar{e}_M\|^2$ and $g_{ii}\|\bar{e}_i\|^2$ for $i = 1 \sim 3$ if the scale factor r is chosen such as $r = 0.02 \sim 0.03$. Then, we define

$$E = K + \tilde{P} - P_\infty, \quad W(\alpha) = E - \alpha V \tag{A-16}$$

where $\alpha > 0$ is a constant parameter determined later. Then, from Eqs. (A-15) and (A-16) it follows that

$$\left(1 + \frac{\alpha}{2}\right)E \geq W(\alpha) \geq \left(1 - \frac{\alpha}{2}\right)E \tag{A-17}$$

Next, note that Eq. (A-5) can be rewritten in the form

$$-B\Delta \boldsymbol{m} + \boldsymbol{d}_N = \frac{\Delta M g}{2}\bar{e}_M + \sum_{i=1}^{3}\sum_{j=1}^{3} g_{ij}\Delta p_j \bar{e}_j / r_j + \sum_{i=1}^{3}\sum_{j=1}^{3} O_{ij}(\|\Delta \boldsymbol{p}\|^2)\bar{e}_j / r_j \tag{A-18}$$

where $r_3 = 0.1$, $O_{ij}(\|\Delta \boldsymbol{p}\|^2)$ is of order $g_m\|\Delta p\|^2$ with $g_m > 0$, and g_m is of order of the maximum eigenvalue of matrix G. Then, it is possible to evaluate the derivative of $W(\alpha)$ in t, which results in

$$\begin{aligned}\frac{\mathrm{d}}{\mathrm{d}t}W(\alpha) &= \frac{\mathrm{d}}{\mathrm{d}t}E - \alpha\frac{\mathrm{d}}{\mathrm{d}t}V \\ &= -\sum_{i=1,2} c_i\|\dot{\boldsymbol{q}}_i\|^2 - \alpha\{\ddot{z}^{\mathrm{T}} H \boldsymbol{w} + \dot{z}^{\mathrm{T}}\dot{H}\boldsymbol{w} + \dot{z}^{\mathrm{T}} H \dot{\boldsymbol{w}}\} \\ &= -\sum_{i=1,2} c_i\|\dot{\boldsymbol{q}}_i\|^2 + \alpha\{\boldsymbol{w}^{\mathrm{T}}(B\Delta \boldsymbol{m} - \boldsymbol{d}_N) \\ &\quad - \boldsymbol{w}^{\mathrm{T}} C\dot{z} + h(\dot{z})\boldsymbol{w} + \dot{z}^{\mathrm{T}} H \dot{\boldsymbol{w}}\}\end{aligned} \tag{A-19}$$

where the relation of Eq. (A-8) is taken into account and $h(\dot{z})$ is a vector composed of quadratic functions of components of $\dot{z}$. By substituting Eqs. (A-9) and (A-18) into Eq. (A-19), we obtain

$$\begin{aligned}\frac{\mathrm{d}}{\mathrm{d}t}W(\alpha) \leq &-\sum_{i=1,2} c_i\|\dot{\boldsymbol{q}}_i\|^2 - \alpha \boldsymbol{w}^{\mathrm{T}} C\dot{z} \\ &- \alpha\left\{\frac{2\bar{e}_M^{\mathrm{T}} P_M \bar{e}_M}{\sqrt{\gamma_M}\|\bar{e}_M\|^2}\cdot\frac{\gamma_M}{2}\Delta M^2 g + \sum_{i=1}^{3}\frac{\bar{e}_i^{\mathrm{T}} P_i \bar{e}_i}{r_i\|\bar{e}_i\|^2}\cdot g_{ii}\Delta p_i^2\right\} \\ &+ \alpha\{O(\|\dot{z}\|^2)(\|\boldsymbol{w}\| + 1)h_M\}\end{aligned} \tag{A-20}$$

where h_M denotes the maximum eigenvalue of H defined in Eq. (A-2). Finally, note that

$$\begin{aligned}-\boldsymbol{w}^{\mathrm{T}} C\dot{z} &\leq \frac{1}{2}\sum_{i=1,2} c_i\|\dot{\boldsymbol{q}}_i\|^2 + \frac{c_M}{2}\|\boldsymbol{w}\|^2 \\ &\leq \sum_{i=1,2}\frac{c_i}{2}\|\dot{\boldsymbol{q}}_i\|^2 + \frac{c_M}{2}\left\{\frac{\bar{e}_M^{\mathrm{T}} P_M \boldsymbol{e}_M}{\|\bar{e}_M\|^4}\gamma_M \Delta M^2 + \sum_{i=1}^{3}\frac{\bar{e}_i^{\mathrm{T}} P_i \bar{e}_i}{\|\bar{e}_i\|^4}\Delta p_i^2\right\}\end{aligned} \tag{A-21}$$

where $c_M = \max(c_1, c_2)$. Then, substituting Eq. (A-21) into Eq. (A-20) yields

$$\begin{aligned}\frac{\mathrm{d}}{\mathrm{d}t}W(\alpha) \leq &-\sum_{i=1,2}\frac{c_i}{2}\|\dot{\boldsymbol{q}}_i\|^2 \\ &- \alpha\left\{\left(\frac{2g}{\sqrt{\gamma_M}} - \frac{c_M}{\|\bar{e}_M\|^2}\right)\xi_M\cdot\frac{\gamma_M}{2}\Delta M^2 \right. \\ &\left. + \sum_{i=1}^{3}\left(\frac{1}{r_i} - \frac{c_M/2}{g_{ii}\|\bar{e}_i\|^2}\right)\xi_i\cdot g_{ii}\Delta p_i^2\right\} \\ &+ \alpha\{O(\|\dot{z}\|^2)(\|\boldsymbol{w}\| + 1)h_M\}\end{aligned} \tag{A-22}$$

where we set

$$\xi_M = \frac{\bar{e}_M^{\mathrm{T}} P_M \bar{e}_M}{\|\bar{e}_M\|^2}, \quad \xi_i = \frac{\bar{e}_i^{\mathrm{T}} P_i \bar{e}_i}{\|\bar{e}_i\|^2} \tag{A-23}$$

https://doi.org/10.1017/S0263574707003840 Published online by Cambridge University Press

According to Tables 3 and 4, it can be easily concluded that

$$\frac{2g}{\sqrt{\gamma_M}} - \frac{c_M}{\|\bar{\boldsymbol{e}}_M\|^2} \geq \frac{g}{\sqrt{\gamma_M}} \tag{A-24}$$

$$\frac{1}{r_i} - \frac{c_M}{2g_{ii}\|\bar{\boldsymbol{e}}_i\|^2} \geq \frac{1}{2r_i}, \qquad i = 1, 2, 3 \tag{A-25}$$

Thus, if ξ_M and ξ_i $(i = 1, 2, 3)$ satisfy

$$\frac{g}{\sqrt{\gamma_M}}\xi_M > 1, \quad \frac{\xi_i}{2r_i} > 1 \quad (\text{for } i = 1, 2, 3) \tag{A-26}$$

for all $t \geq 0$, then Eq. (A-22) can be written as

$$\frac{\mathrm{d}}{\mathrm{d}t}W(\alpha) \leq -\sum_{i=1,2}\frac{c_i}{2}\|\dot{\boldsymbol{q}}_i\|^2 - \alpha\left\{\frac{\gamma_M}{2}\Delta M^2 + \sum_{i=1}^{3} g_{ii}\Delta p_i^2\right\} + \alpha\{O(\|\dot{\boldsymbol{z}}\|^2)(\|\boldsymbol{w}\|+1)h_M\} \tag{A-27}$$

At this stage, note that in a similar argument to that in derivation of Eq. (A-14) it is possible to verify that

$$\begin{aligned}&\frac{\gamma_M}{2}\Delta M^2 + \sum_{i=1}^{3} g_{ii}\Delta p_i^2 \\ &\geq \frac{\gamma_M}{2}\Delta M^2 + \frac{1}{2}\sum_{i,j} g_{ij}\Delta p_i \Delta p_j + O(\|\Delta \boldsymbol{p}\|^3) \\ &\geq \tilde{P} - \tilde{P}_\infty + O(\|\Delta \boldsymbol{p}\|^2)\end{aligned} \tag{A-28}$$

Finally, it should be remarked that from the four velocity constraints $\dot{Q}_i = 0$ and $\dot{R}_i = 0$ for $i = 1, 2$ it follows that[4,5]

$$r^{-2}(\dot{x}^2 + \dot{y}^2) + \dot{\theta}^2 \leq O\left(\sum_{i=1,2}\|\dot{\boldsymbol{q}}_i\|^2\right) \tag{A-29}$$

Since h_M is far less than c_i $(i = 1, 2)$, that is, h_M is of $O(10^{-5})$ and c_i is of $O(10^{-3})$ $(i = 1, 2)$,

$$\begin{aligned}&-\sum_{i=1,2}\frac{c_i}{2}\|\dot{\boldsymbol{q}}_i\|^2 + \alpha\{O(\|\dot{\boldsymbol{z}}\|^2)(\|\boldsymbol{w}\|+1)h_M\} \\ &\leq -\frac{\alpha}{2}\dot{\boldsymbol{z}}^{\mathrm{T}} H \dot{\boldsymbol{z}} = -\alpha K\end{aligned} \tag{A-30}$$

as far as $\alpha \leq 1.0$. By substituting Eqs. (A-28) and (A-30) into Eq. (A-27), it is now concluded that

$$\frac{\mathrm{d}}{\mathrm{d}t}W(\alpha) \leq -\alpha(K + \tilde{P} - P_{0\infty}) = -\alpha E \tag{A-31}$$

which implies, from Eq. (A-17), that

$$\frac{\mathrm{d}}{\mathrm{d}t}W(\alpha) \leq -\alpha E \leq \frac{-2\alpha}{2+\alpha}W(\alpha) \tag{A-32}$$

In particular, set $\alpha = 1$ and denote the value of $W(1)$ at time t by $W(t)$. Then, Eq. (A-32) yields

$$W(t) \leq e^{-(2/3)t}W(0) \tag{A-33}$$

which leads to

$$\begin{aligned}E(t) &\leq 2W(t) \leq 2e^{(-2/3)t}W(0) \\ &\leq 3e^{(-2/3)t}E(0)\end{aligned} \tag{A-34}$$

This shows exponential convergences of $\dot{z}(t)$ to zero, and $\Delta \boldsymbol{p}$ to zero and ΔM to zero. Thus, the force/torque balance is established asymptotically in an exponential speed of convergence.

Before closing the proof, it should be remarked that the inequality condition of (A-25) for $i = 3$ is equivalent to

$$c_M / g_{33} r_3 \leq 1 \tag{A-35}$$

which can be expressed approximately by referring to Eq. (57a) as

$$r_3 = \frac{c_M}{f_d(r_1 + r_2)\cos^2\theta_0} = 0.1 \sim 0.3 \tag{A-36}$$

Such a choice of parameter r_3 is feasible if damping factors c_i for finger joints are chosen in such a way that

$$c_1 = c_2 = r_3 f_d(r_1 + r_2) \tag{A-37}$$

with $r_3 = 0.1 \sim 0.3$ [s^{-1}]. This rule of thumb for adequate choice of finger joint damping factors was recommended in the previous paper[15] by referring to Hill's model of force/torque characteristics of muscle contraction.

https://doi.org/10.1017/S0263574707003840 Published online by Cambridge University Press